Pretreatment with Haloperidol Reduces ^{123}I-FP-CIT Binding to the Dopamine Transporter in the Rat Striatum: An In Vivo Imaging Study with a Dedicated Small-Animal SPECT Camera

Susanne Nikolaus, Christina Antke, Konstantin Kley, Markus Beu, Andreas Wirrwar, and Hans-Wilhelm Müller

Clinic of Nuclear Medicine, University Hospital Düsseldorf, Düsseldorf, Germany

Synaptic dopamine is mainly regulated by presynaptic dopamine transporter (DAT) activity. We hypothesized that variations in synaptic dopamine are reflected by variations of DAT radioligand binding. The effect of haloperidol, which increases synaptic dopamine concentrations, was therefore assessed in the rat striatum using ^{123}I-*N*-ω-fluoropropyl-2β-carbomethoxy-3β-(4-iodophenyl)-nortropane (^{123}I-FP-CIT) as a DAT radioligand. **Methods:** Striatal ^{123}I-FP-CIT binding was measured in 24 rats under baseline conditions (no pretreatment) and at 1 h after injection of haloperidol or a vehicle (1 mg/kg) using a small-animal SPECT camera. **Results:** Baseline equilibrium ratios (V_3'') were 1.32 ± 0.24 (mean ± SD). After the haloperidol injection, V_3'' decreased to 0.99 ± 0.38 ($P_{2\text{-tailed}} < 0.0001$), corresponding to a mean reduction of DAT binding by 25%. **Conclusion:** Our results are indicative of competition between the DAT ligand ^{123}I-FP-CIT and synaptic dopamine elevated by haloperidol, suggesting that the assessment of ^{123}I-FP-CIT binding may be suitable to study variations in synaptic dopamine in vivo.

Key Words: FP-CIT; haloperidol; dopamine transporter; molecular imaging; small-animal SPECT

J Nucl Med 2009; 50:1147–1152
DOI: 10.2967/jnumed.109.061952

Antipsychotic drugs such as the neuroleptic haloperidol are known to increase the synthesis and release of dopamine in the striatum and related mesolimbic structures (*1–4*). The suggested mechanism of action is the blockade of terminal presynaptic autoreceptors (*2*), leading to an abolition of feedback inhibition and, thus, to an increase of dopamine synthesis or release. Accordingly, compartmental analysis of 3-*N*-^{11}C-methylspiperone binding in pigs showed that the application of haloperidol led to antagonist binding to postsynaptic D_2 receptors and then to increased availability of endogenous dopamine, both resulting in a reduction of exogenous ligand binding to postsynaptic D_2 receptors in the striatum (*5*).

In this study, we pursue an analogous approach to the presynaptic constituent of the dopaminergic synapse using the tropane analog ^{123}I-*N*-ω-fluoropropyl-2β-carbomethoxy-3β-(4-iodophenyl)-nortropane (^{123}I-FP-CIT), which binds to the presynaptic dopamine transporter (DAT). Clinically, ^{123}I-FP-CIT is used for the differential diagnosis between idiopathic Parkinson disease (Parkinsonian patients show a reduction of striatal DAT binding) and essential tremor (DAT is no different in individuals with essential tremor DAT vs. healthy controls) (*6*). If endogenous dopamine displaces exogenous radioligands or competes with them for presynaptic binding sites, this may have implications for DAT imaging studies in Parkinsonian subjects, who are treated with pharmacologic compounds that lead to an increased availability of dopamine in the synaptic cleft. Moreover, DAT binding is increasingly assessed in schizophrenic patients (*7–16*). Because neuroleptics such as haloperidol increase endogenous dopamine concentrations, radioligand binding to the DAT may be severely confounded in medicated schizophrenic patients.

In recent investigations, we demonstrated that DAT and D_2 receptor binding and blockade with methylphenidate and haloperidol, respectively, may be quantified in vivo in the rat striatum using a dedicated small-animal SPECT device (*17–20*). Additionally, it was shown that increases of synaptic dopamine as induced by methylphenidate may be assessed by quantifying D_2 receptor binding successively under pre- and posttreatment conditions (*18*). Here we investigate the effect of haloperidol, that is, the increase of synaptic dopamine on ^{123}I-FP-CIT binding to the presynaptic DAT. Striatal DAT binding was measured in the rat under baseline conditions and at 1 h after pretreatment with haloperidol or a vehicle.

Received Jan. 12, 2009; revision accepted Mar. 16, 2009.
For correspondence or reprints contact: Susanne Nikolaus, University Hospital Düsseldorf, Moorenstrasse 5, Düsseldorf, Germany D-40225.
E-mail: Susanne.Nikolaus@uni-duesseldorf.de

MATERIALS AND METHODS

Animals

DAT imaging studies were performed on 24 adult male Wistar rats (TVA, Heinrich-Heine University) weighing 442 ± 51 g (mean ± SD). On 3 other animals, images of bone metabolism, soft-tissue perfusion, and brain perfusion were acquired to delineate the striatal and cerebellar target regions, as previously published (*17,20*). Animals were maintained under standard laboratory conditions, with food and water freely available. The study was approved by the regional authority; it was performed in accordance with the Principles of Laboratory Animal Care (*21*) and the German Law on the Protection of Animals.

SPECT Camera

The small-animal tomograph (TierSPECT; Central Institute for Electronics [Zel]) used in this study was described in detail elsewhere (*22*). The tomographic spatial resolution (full width at half maximum) of this camera was 3.4 mm for ^{123}I (distance, 30 mm), and the sensitivity was 16 cps/MBq. Data were acquired in a 128 × 128 matrix (pixel width and slice thickness, ≈0.664 mm). Reconstruction was performed using an iterative ordered-subset expectation maximization algorithm (3 iterations, 4 subsets per iteration). No postfiltering procedure was applied. Attenuation correction was implemented, assuming a uniformly attenuating medium (linear attenuation coefficient, 0.10 cm^{-1}).

Experimental Protocol

In all animals, DAT binding was assessed under baseline conditions (no treatment) and after pretreatment with haloperidol or a vehicle. Investigations were performed in randomized order, 10 ± 7 d apart. For baseline measurements, animals were intraperitoneally administered a mixture of ketamine hydrochloride (0.9 mL/kg; Ketavet [Pharmacia GmbH]) (concentration, 100 mg/mL) and xylazine hydrochloride (0.4 mL/kg; Rompun [Bayer]) (concentration, 20 mg/mL). ^{123}I-FP-CIT (27 ± 6 MBq; DaTSCAN [GE Healthcare]) (concentration range, 0.07–0.13 μg/mL; specific activity range, 2.5–4.5 × 10^{14} Bq/mmol at reference time) was injected into the lateral tail vein using a winged infusion needle set. The tube was rinsed with 1 mL of 0.9% saline, amounting to a total injection volume of 1.3 mL.

According to Hume et al. (*23*), a DAT occupancy of less than 5% may be expected with an applied mean radioactivity of 27 MBq, a mean animal weight of 442 g, a mean specific activity of 3.5 × 10^{14} Bq/mmol, and an inhibition constant of 3.5 nmol/L (*24*). In vivo microdialysis studies have shown that maximum striatal dopamine concentrations are reached between 60 and 90 min after intraperitoneal application of haloperidol and remain stable for at least 2 h (*3*). Thus, animals received intraperitoneal injections of either haloperidol (Sigma-Aldrich) (1 mg/kg; concentration, 1 mg/mL) or vehicle (ethanol, 1 mg/kg; concentration, 100 mg/mL) 1 h before radioligand application. A total of 20 of 24 rats underwent the baseline measurement and measurement after haloperidol challenge, and 10 of 24 rats underwent the baseline measurement and measurement after injection of vehicle. Thereby, of the 20 rats that were subjected to both the baseline measurement and the measurement after pretreatment with haloperidol, 13 rats were measured twice; 7 rats also underwent a third measurement after pretreatment with vehicle.

For SPECT measurements, animals were positioned in a custom-built head holder (Institute of Medicine) to ensure reproducible positioning of the animals. Previous investigations on rats have shown that equilibrium of ^{123}I-FP-CIT binding is reached at 2 h after injection, with the ratio of specific-to-nonspecific striatal uptake remaining stable through the following 4 h (*25*). Thus, SPECT measurements were started 2 h after radioligand application. Imaging data were acquired for 60 min in a step-and-shoot mode over a circular orbit in angular steps of 6° (60 projections, 60 s/projection), using a 65-mm radius of rotation. The 15% energy window was centered on the 159-keV γ-photopeak of ^{123}I.

Imaging of head and neck bone metabolism, head and neck soft-tissue perfusion, and brain perfusion was performed as previously described using ^{99m}Tc-3,3-diphosphono-1,2-propandeicarboxylic acid (^{99m}Tc-DPD) (Teceos; CIS Diagnostik), ^{99m}Tc-tetrofosmin (Myoview; Amersham Buchler), and ^{99m}Tc-hexamethylpropyleneamine oxime (^{99m}Tc-HMPAO) (Ceretec; Amersham Buchler) as radiotracers (*17,20*). Imaging data were recorded as described above. The 15% energy window was centered on the 140-keV γ-photopeak of ^{99m}Tc.

Evaluation

Imaging data were evaluated using the Multi-Purpose-Imaging-Tool (Advanced Tomo Vision GmbH) as previously described (*17,20*). Briefly, target and reference regions were identified using sets of fusion images (^{99m}Tc-DPD–^{99m}Tc-tetrofosmin, ^{99m}Tc-DPD–^{99m}Tc-HMPAO, and ^{99m}Tc-DPD–^{123}I-FP-CIT), allowing the detection of extracerebral anatomic landmarks such as the cranium, orbitae, and Harderian glands and the localization of the respective regions relative to the sites of specific accumulation of metabolism and perfusion markers. Maximum striatal and cerebellar counting rates (counts per pixel) were determined on coronal slices. Thereby, cerebellar counting rates were obtained in an elliptic region approximately 15 mm posterior to the frontal cortex, corresponding anatomically to the rat cerebellum (*26*). Additionally, the position of the cerebellum was verified visually with ^{99m}Tc-DPD–^{123}I-FP-CIT fusion images.

The equilibrium ratio of the distribution volumes of the specifically and the nonspecifically bound compartment ($V_3'' = V_3/V_2$) was computed as an estimate for the binding potential (*27*). V_3'' can be obtained as $(V_T/V_2) - 1$, with V_T denoting the total tissue equilibrium volume of distribution, equal to the sum of V_2 and V_3. If it is assumed that the equilibrium concentrations of free and nonspecifically bound ligand are the same across brain regions, V_2 may be inferred from a region devoid of the target receptor (e.g., cerebellum), and V_3'' in the striatum is obtained as V_T(striatum)/V_T(cerebellum) – 1.

Statistical Analysis

For baseline and treatment conditions, striatal V_3'' values were obtained from radioactivity concentrations (counts per pixel) in striatal target and cerebellar reference regions. Left and right striatal radioactivity concentrations were averaged. Cerebellar counting rates were normalized to the injected radioactivity (MBq) divided by the weight of the respective animal (g). The normal distribution of data was ascertained for each condition with the nonparametric Kolmogorov–Smirnov test ($0.394 < P < 0.993$).

Striatal V_3'' values were compared between pretreatment conditions (baseline, pretreatment with haloperidol, and pretreatment with vehicle) with both 1-way ANOVA and paired *t* tests (2-tailed). Moreover, to test for possible influences of haloperidol on nonspecific binding (e.g., due to effects on perfusion) cerebellar counting rates were compared between pretreatment conditions (baseline, pretreatment with haloperidol, and pretreatment with vehicle) with the paired *t* test (2-tailed).

RESULTS

A typical example of cerebral ^{123}I-FP-CIT accumulation is shown in Figure 1. Figure 1A displays a characteristic coronal slice of a rat's brain measured under baseline conditions. Prominent is the radioligand accumulation in the paired striatum. Figure 1B shows the ^{123}I-FP-CIT accumulation in the same rat after pretreatment with haloperidol. Reduction of striatal ^{123}I-FP-CIT binding is evident.

Striatal ^{123}I-FP-CIT binding data of all investigated animals are presented in Figure 2.

Under the baseline condition and after pretreatment with a vehicle, the animals yielded striatal V_3'' values of 1.32 ± 0.24 and 1.49 ± 0.37, respectively. After pretreatment with haloperidol, V_3'' values decreased to 0.99 ± 0.38. The 1-way ANOVA yielded a significant effect of treatment ($P < 0.0001$).

No significant difference between baseline condition and pretreatment with a vehicle ($n = 10$; paired t test, 2-tailed, $P = 0.360$) was observed. The differences between pretreatment with haloperidol and both baseline levels and levels under a vehicle were significant (baseline vs. haloperidol: $n = 20$; paired t test, 2-tailed, $P < 0.0001$; and haloperidol vs. vehicle: $n = 7$, paired t test, 2-tailed, $P = 0.010$).

Group comparisons between baseline levels and levels under pretreatment with haloperidol were also performed separately for the 13 rats undergoing 2 investigations and the 7 rats undergoing 3 investigations. The difference between baseline condition and pretreatment with haloperidol remained significant, irrespective of the number of investigations (2 measurements: paired t test, 2-tailed, $P = 0.005$; and 3 measurements: paired t test, 2-tailed, $P = 0.018$).

Decreases of DAT binding were observed in 16 of 20 animals (32% ± 19%), and increases of DAT binding were shown in 4 of 20 animals (5.4% ± 2.8%).

Cerebellar uptake values of ^{123}I-FP-CIT were 13,561 ± 2,847 ($\frac{\text{counts/pixel}}{\text{MBq}} \times$ g; baseline), 11,666 ± 4,375 (vehicle), and 15,078 ± 4,405 (haloperidol; data not shown). Differences between baseline and pretreatment with haloperidol and between baseline and pretreatment with vehicle were not significant ($P = 0.309$ and 0.271, respectively).

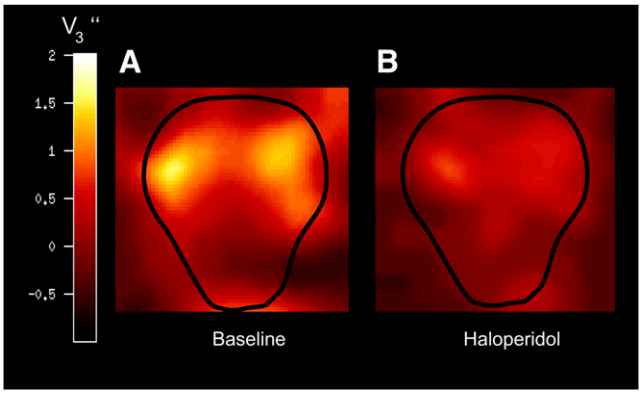

FIGURE 1. Characteristic slices of rat head under baseline conditions (A) and after pretreatment with haloperidol (B). Images show V_3'' values within cerebral outline. Calculations were performed using MATLAB (version 4.2c; The MathWorks Inc.). Reduction in striatal ^{123}I-FP-CIT binding is evident and in this animal amounts to 54%.

DISCUSSION

In this in vivo imaging study, pretreatment with haloperidol (1 mg/kg) induced a mean reduction of 25% of striatal ^{123}I-FP-CIT binding relative to baseline, suggesting a competition between ^{123}I-FP-CIT and endogenous dopamine.

Among the methodologic issues that warrant consideration are the use of ketamine as an anesthetic and the use of ethanol as a solvent for haloperidol. It may be dismissed, however, that the effect on ^{123}I-FP-CIT binding was due to anesthesia, because animals were subjected to the same anesthesia protocol in both control and treatment conditions. Furthermore, in the present investigation, ethanol did not

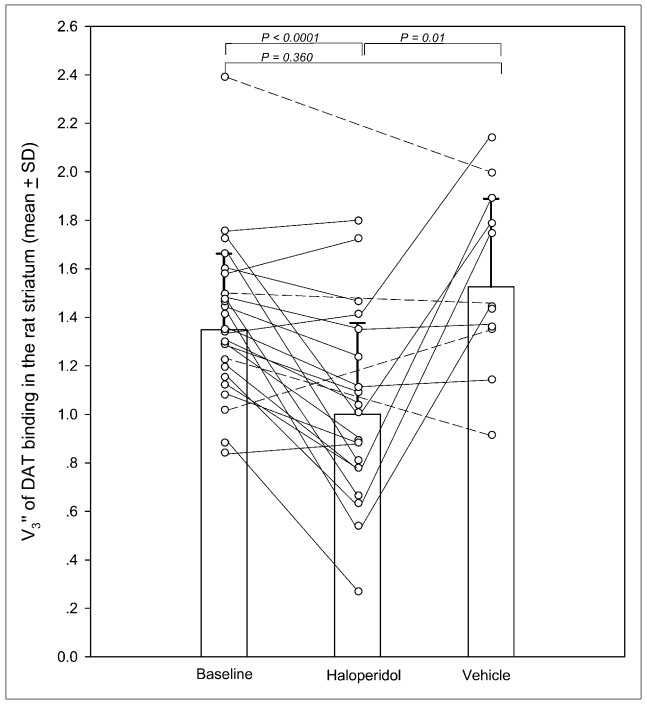

FIGURE 2. V_3'' under baseline conditions and after pretreatment with haloperidol and vehicle. Circles represent individual animals. V_3'' values obtained for each rat on different days are connected by dotted lines. Investigated were total of 24 rats; thereby, 20 rats underwent baseline measurement and measurement after haloperidol challenge (solid lines), and 4 rats were subjected to baseline measurement and measurement after application of vehicle without assessment of DAT binding after challenge with haloperidol (dashed lines). V_3'' values were compared between conditions using paired t test (2-tailed). Differences between baseline and haloperidol and between haloperidol and vehicle were significant. Exclusion of animal with highest V_3'' value at baseline (left column) leaves P value for comparisons between baseline and haloperidol unaltered. Difference between baseline and pretreatment with vehicle remains nonsignificant ($P = 0.18$).

significantly affect specific striatal DAT binding; thus, it may be excluded that the solvent on its own produced any effect by increasing dopamine concentrations in the synaptic cleft. Moreover, cerebellar radioactivity concentrations did not differ between baseline and pretreatment with ethanol or between baseline and pretreatment with haloperidol, demonstrating that, under the present experimental conditions, neither ethanol nor haloperidol exerted confounding effects on radioligand accumulation (e.g., by affecting cerebral perfusion).

Another issue is the time point of haloperidol administration relative to the time point of radioligand application. Previous in vivo microdialysis studies showed that maximum striatal dopamine concentrations are reached between 60 and 90 min after intraperitoneal or intravenous injection of haloperidol (*1,3*). In the present study, haloperidol was injected 60 min before ^{123}I-FP-CIT application. Thus, the radioligand was administered at the time when maximum striatal dopamine concentrations were reached (*1,3*). ^{123}I-FP-CIT requires 2 h to reach the state of equilibrium (*25*). Because striatal dopamine concentrations remain stable for 2 h (*25*), there is sufficient time for ^{123}I-FP-CIT to reach a binding equilibrium in competition with endogenous dopamine. Moreover, previous investigations have shown that the ratio of specific-to-nonspecific striatal ^{123}I-FP-CIT uptake remains stable for 4 h (*25*). Therefore, a suitable time window for the assessment of ^{123}I-FP-CIT binding in relation to increase of endogenous dopamine is between 2 and 3 h.

Furthermore, the possibility must be considered that either haloperidol or its metabolites directly competed with the exogenous ligand for DAT binding sites. In vitro studies provided no evidence that haloperidol or its metabolites have an affinity for the DAT (haloperidol: inhibition constant [K_i], 5,100 nM; metabolites: 2,600–6,800 nM) (*28*). In vivo investigations on baboons, however, showed that chronic pretreatment with the tetrahydropyridine metabolite 4-(4-chlorophenyl)-1-[4-(4-fluorophenyl)-4-oxobutyl]-1,2,3,6-tetrahydropyridine reduced both ^{123}I-iodobenzamide and ^{123}I-2β-carbomethoxy-3β-(4-iodophenyl)tropane binding in the basal ganglia and cerebellum (*29*). Thus, it may not be generally ruled out that metabolites also, to some extent, contributed to the reduction of striatal ^{123}I-FP-CIT binding after pretreatment with haloperidol by interacting with either pre- or postsynaptically located binding sites. However, with a comparatively low inhibitory concentration of 50% of 12,000 nM, this is not likely. Additionally, only chronic exposure to haloperidol could have resulted in brain levels of the quaternary pyridinium species sufficient to induce irreversible depletion of striatal dopamine and DAT binding sites.

Our assumption that haloperidol induced an increase of synaptic dopamine is supported by the following lines of evidence: First, neuroleptics have repeatedly been shown to increase the synthesis, metabolism, and release of dopamine in the striatum and related mesolimbic structures (*1–5*).

Second, various mechanisms have already been suggested by which haloperidol can be assumed to act on synaptic dopamine. For one, the effect of haloperidol can be mediated by the D_2 antagonist binding to terminal presynaptic autoreceptors. Autoreceptor blockade then leads to an abolition of feedback inhibition and thus to an increase of dopamine synthesis or dopamine release (*2*). Moreover, as a result of concurrent autoreceptor regulation, a downregulation of dopamine reuptake (in addition to an upregulation of dopamine release) has been also observed, which likewise leads to an increased availability of dopamine in the synaptic cleft (*4*). On the other side, haloperidol may bind to postsynaptic D_2 receptors, with postsynaptic D_2 receptor blockade also leading to an increased availability of endogenous dopamine via an indirect neuronal feedback mechanism (*30*). The lesion studies by Westerink and de Vries have shown that postsynaptic binding to dopaminergic nerve terminals is not involved in the neuroleptic-induced increase in dopamine release, which also holds for neuroleptic binding to D_2 autoreceptors on soma and dendrites (*31*). Therefore, our results are most likely to reflect haloperidol-induced stimulation of dopamine release via the terminal presynaptic D_2 autoreceptor binding site or inhibition of dopamine reuptake via the DAT binding site.

Third, our in vivo findings on rats are supported by previous in vivo and ex vivo studies, which provided evidence that the application of the dopamine-releasing agents amphetamine and L-3,4-dihydroxyphenylalanine may lead to a reduction of exogenous radioligand binding to the DAT (*32,33*). Findings are furthermore in line with evidence presented by the Parkinson Study Group (*34*), which demonstrated a greater (though nonsignificant) decrease in striatal ^{123}I-FP-CIT binding in patients treated with levodopa, compared with placebo-treated controls. Results are of particular interest with regard to scientific investigations of DAT binding in Parkinsonian subjects receiving any treatment—be it antioxidative, neuroprotective, or surgical—that leads to increased availabilities of synaptic dopamine.

In vivo microdialysis studies in rats showed a 50% increase of endogenous dopamine after a 1 mg/kg dose of haloperidol (*3*). This increase of endogenous dopamine, in context with our findings, poses the question of whether an increase of dopamine of this order of magnitude is sufficient to enter into an effective competition with the exogenous DAT ligand. So far, to our knowledge, the dissociation constant of ^{123}I-FP-CIT has not been experimentally determined. The K_i value, however, is known and amounts to 3.5 nM under competition with GBR12909 (*23*). For dopamine, an inhibitory concentration of 50% of 3.7 nM (*35*) and K_i values between 0.59 and 19 nM (*36*) were reported using GBR12909 and WIN 35,065 analogs, respectively, as competitors. However, K_i values in the micromolar range also were obtained when unlabeled dopamine was used as a competitor (*37*). This merely allows for a tentative estimation of binding relations at the presynaptic terminal. If the affinities of exogenous and endogenous ligands lie within the same order of magnitude, it is conceivable that the observed 25% decrease of ^{123}I-FP-CIT binding reflects a

25% increase of synaptic dopamine. If, however, the affinity of ^{123}I-FP-CIT for the DAT is, for example, one order of magnitude higher than the affinity of dopamine, a 25% decrease of ^{123}I-FP-CIT binding would reflect an increase of synaptic dopamine by 10-fold. This increase is not consistent with the findings of Pehek (*3*), who showed a 50% increase of endogenous dopamine using in vivo microdialysis. Thus, further investigations are needed that explicitly address the quantification of synaptic dopamine.

Recently, there has been growing interest in assessing DAT binding in schizophrenic patients. Results on striatal DAT binding in schizophrenic subjects have been inconsistent, with reports of either elevated (*11,12*), reduced (*9,11,16*), or unaltered (*7,8,10,13–15*) DAT binding. Interestingly, also in medicated patients, either unaltered (*8*), decreased (*9,16*), or increased DAT binding (*12*) has been observed. Results are difficult to interpret because factors such as duration of illness and illness phase, which may vary between patients and between investigations, are likely to affect the regulation state of pre- and postsynaptic binding sites. Our findings, moreover, suggest that neuroleptic medication itself may confound presynaptic binding data. It is known that schizophrenic patients who are not responding to neuroleptic treatment may present with a high percentage of occupied D_2 receptors and, nevertheless, display no relief of symptoms (*38*). In the light of the present findings, it is conceivable that presynaptic autoreceptor or transporter function may be dysregulated in this subgroup of schizophrenic patients. In addition, in the present study haloperidol pretreatment did not induce a reduction of DAT binding in all of the investigated animals, underlining the importance of further investigation of haloperidol-induced effects on dopamine release and presynaptic binding sites in preclinical animal models or schizophrenic patients.

CONCLUSION

In this study, the effect of haloperidol on DAT binding was assessed in the rat striatum using ^{123}I-FP-CIT as a radioligand. Pretreatment with a 1 mg/kg dose of haloperidol induced a 25% reduction of DAT binding relative to baseline. Results in the rat striatum are indicative of the competition between the dopamine transporter ligand ^{123}I-FP-CIT and synaptic dopamine elevated by haloperidol and, thus, suggest that assessment of ^{123}I-FP-CIT binding may be suitable to study variations in synaptic dopamine. This may be of particular interest for investigating the interrelation of synaptic dopamine and DAT function in schizophrenia and other diseases known to be associated with presynaptic deficiencies, such as attention-deficit hyperactivity disorder and Parkinson disease.

REFERENCES

1. Moghaddam B, Bunney BS. Acute effects of typical and atypical antipsychotic drugs on the release of dopamine from prefrontal cortex, nucleus accumbens, and striatum of the rat: an in vivo microdialysis study. *J Neurochem.* 1990;54:1755–1760.
2. Pehek EA, Yamamoto BK. Differential effects of locally administered clozapine and haloperidol on dopamine efflux in the rat prefrontal cortex and caudate-putamen. *J Neurochem.* 1994;63:2118–2124.
3. Pehek EA. Comparison of effects of haloperidol administration on amphetamine-stimulated dopamine release in the rat medial prefrontal cortex and dorsal striatum. *J Pharmacol Exp Ther.* 1999;289:14–23.
4. Wu Q, Reith ME, Walker QD, Kuhn CM, Carroll FI, Garris PA. Concurrent autoreceptor-mediated control of dopamine release and uptake during neurotransmission: an in vivo voltammetric study. *J Neurosci.* 2002;22:6272–6281.
5. Ishizu K, Smith DF, Bender D, et al. Positron emission tomography of radioligand binding in porcine striatum in vivo: haloperidol inhibition linked to endogenous ligand release. *Synapse.* 2000;38:87–101.
6. Scherfler C, Schwarz J, Antonini A, et al. Role of DAT-SPECT in the diagnostic work up of parkinsonism. *Mov Disord.* 2007;22:1229–1238.
7. Laruelle M, Abi-Dargham A, van Dyck C, et al. Dopamine and serotonin transporters in patients with schizophrenia: an imaging study with [^{123}I]β-CIT. *Biol Psychiatry.* 2000;47:371–379.
8. Laakso A, Vilkman H, Alakare B, et al. Striatal dopamine transporter binding in neuroleptic-naive patients with schizophrenia studied with positron emission tomography. *Am J Psychiatry.* 2000;157:269–271.
9. Laakso A, Bergman J, Haaparanta M, et al. Decreased striatal dopamine transporter binding in vivo in chronic schizophrenia. *Schizophr Res.* 2001;52:115–120.
10. Lavalaye J, Linszen DH, Booij J, et al. Dopamine transporter density in young patients with schizophrenia assessed with [123]FP-CIT SPECT. *Schizophr Res.* 2001;47:59–67.
11. Hsiao MC, Lin KJ, Liu CY, Tzen KY, Yen TC. Dopamine transporter change in drug-naive schizophrenia: an imaging study with ^{99m}Tc-TRODAT-1. *Schizophr Res.* 2003;65:39–46.
12. Sjoholm H, Bratlid T, Sundsfjord J. ^{123}I-β-CIT SPECT demonstrates increased presynaptic dopamine transporter binding sites in basal ganglia in vivo in schizophrenia. *Psychopharmacology (Berl).* 2004;173:27–31.
13. Yang YK, Yu L, Yeh TL, Chiu NT, Chen PS, Lee IH. Associated alterations of striatal dopamine D2/D3 receptor and transporter binding in drug-naive patients with schizophrenia: a dual-isotope SPECT study. *Am J Psychiatry.* 2004;161:1496–1498.
14. Yoder KK, Hutchins GD, Morris ED, Brashear A, Wang C, Shekhar A. Dopamine transporter density in schizophrenic subjects with and without tardive dyskinesia. *Schizophr Res.* 2004;71:371–375.
15. Schmitt GJ, Meisenzahl EM, Frodl T, et al. The striatal dopamine transporter in first-episode, drug-naive schizophrenic patients: evaluation by the new SPECT-ligand [^{99m}Tc]TRODAT-1. *J Psychopharmacol.* 2005;19:488–493.
16. Mateos JJ, Lomena F, Parellada E, et al. Decreased striatal dopamine transporter binding assessed with [^{123}I] FP-CIT in first-episode schizophrenic patients with and without short-term antipsychotic-induced parkinsonism. *Psychopharmacology (Berl).* 2005;181:401–406.
17. Nikolaus S, Wirrwar A, Antke C, et al. Quantitation of dopamine transporter blockade by methylphenidate: first in vivo investigation using [^{123}I]FP-CIT and a dedicated small animal SPECT. *Eur J Nucl Med Mol Imaging.* 2005;32:308–315.
18. Nikolaus S, Larisch R, Wirrwar A, et al. [^{123}I]Iodobenzamide binding to the rat dopamine D_2 receptor in competition with haloperidol and endogenous dopamine: an in vivo imaging study with a dedicated small animal SPECT. *Eur J Nucl Med Mol Imaging.* 2005;32:1305–1310.
19. Nikolaus S, Beu M, Wirrwar A, Antke C, Müller HW. In vivo snapshots of the dopaminergic synapse in small animals. *Mol Psychiatry.* 2005;10:516–518.
20. Nikolaus S, Wirrwar A, Kley K, Antke C, Müller HW. *In vivo* quantification of dose-dependent dopamine transporter blockade in the rat striatum with small animal SPECT. *Nucl Med Commun.* 2007;28:207–213.
21. National Institutes of Health. *Guide for the Care and Use of Laboratory Animals.* NIH Publication No. 86-23. Bethesda, MD: Public Health Service, National Institutes of Health; 1985.
22. Schramm N, Wirrwar A, Sonnenberg F, Halling H. Compact high resolution detector for small animal SPECT. *IEEE Trans Nucl Sci.* 2000;47:1163–1167.
23. Hume SP, Gunn RN, Jones T. Pharmacological constraints associated with positron emission tomographic scanning of small laboratory animals. *Eur J Nucl Med.* 1998;25:173–176.
24. Neumeyer JL, Wang S, Gao Y et al. *N*-ω-fluoroalkyl analogs of (1*R*)-2β-carbomethoxy-3β-(4-iodophenyl)-tropane (β-CIT): radiotracers for positron emission tomography and single photon emission computed tomography imaging of dopamine transporters. *J Med Chem.* 1994;37:1558–1561.
25. Booij J, Andringa G, Rijks LJ, et al. [^{123}I]FP-CIT binds to the dopamine transporter as assessed by biodistribution studies in rats and SPECT studies in MPTP-lesioned monkeys. *Synapse.* 1997;27:183–190.
26. Paxinos G, Watson C. *The Rat Brain in Stereotaxic Coordinates.* Sydney, Australia: Academic Press; 1986.

27. Laruelle M, van Dyck C, Abi-Dargham A, et al. Compartmental modeling of iodine-123-iodobenzofuran binding to dopamine D2 receptors in healthy subjects. *J Nucl Med.* 1994;35:743–754.
28. Bryan-Lluka LJ, Siebert GA, Pond SM. Potencies of haloperidol metabolites as inhibitors of the human noradrenaline, dopamine and serotonin transporters in transfected COS-7 cells. *Naunyn Schmiedebergs Arch Pharmacol.* 1999;360: 109–115.
29. Oliver DW, Dormehl IC, Van der Schyf CJ, et al. Effect of the haloperidol tetrahydropyridine metabolite 4-(4-chlorophenyl)-1-[4-(4-fluorophenyl)-4-oxobutyl]-1,2,3,6-tetrahydropyridine on dopamine receptor and transporter binding: a nonhuman primate ^{123}I-iodobenzamide and 2β-carbomethoxy-3β-(4-iodophenyl)tropane single photon emission computed tomographic study. *Arzneimittelforschung.* 1997;47:692–699.
30. Hommer DW, Bunney BS. Effect of sensory stimuli on the activity of dopaminergic neurons: involvement of non-dopaminergic nigral neurons and striato-nigral pathways. *Life Sci.* 1980;27:377–386.
31. Westerink BHC, de Vries JB. On the mechanism of neuroleptic induced increase in striatal dopamine release: brain dialysis provides direct evidence for mediation by autoreceptors on nerve terminals. *Neurosci Lett.* 1989;99:197–202.
32. Laruelle M, Baldwin M, Malison RT, et al. SPECT imaging of dopamine and serotonin transporters with [^{123}I]β-CIT: pharmacological characterization of brain uptake in nonhuman primates. *Synapse.* 1993;13:295–309.
33. Dresel SH, Kung MP, Plossl K, Meegalla SK, Kung HF. Pharmacological effects of dopaminergic drugs on in vivo binding of [^{99m}Tc]TRODAT-1 to the central dopamine transporters in rats. *Eur J Nucl Med.* 1998;25:31–39.
34. Parkinson Study Group. Dopamine transporter brain imaging to assess the effects of pramipexole vs levodopa on Parkinson disease progression. *JAMA.* 2002; 287:1653–1661.
35. Matecka D, Rothman RB, Radesca L, et al. Development of novel, potent, and selective dopamine reuptake inhibitors through alteration of the piperazine ring of 1-[2-(diphenylmethoxy)ethyl]-and 1-[2-[bis(4-fluorophenyl)methoxy]ethyl]-4-(3-phenylpropyl)piperazines (GBR 12935 and GBR 12909). *J Med Chem.* 1996;39:4704–4716.
36. Kotian P, Mascarella SW, Abraham P, et al. Synthesis, ligand binding, and quantitative structure-activity relationship study of 3 β-(4′-substituted phenyl)-2 β-heterocyclic tropanes: evidence for an electrostatic interaction at the 2 β-position. *J Med Chem.* 1996;39:2753–2763.
37. Lee FJ, Pristupa ZB, Ciliax BJ, Levey AI, Niznik HB. The dopamine transporter carboxyl-terminal tail: truncation/substitution mutants selectively confer high affinity dopamine uptake while attenuating recognition of the ligand binding domain. *J Biol Chem.* 1996;271:20885–20894.
38. Kasper S, Tauscher J, Willeit M, et al. Receptor and transporter imaging studies in schizophrenia, depression, bulimia and Tourette's disorder: implications for psychopharmacology. *World J Biol Psychiatry.* 2002;3:133–146.

The Journal of NUCLEAR MEDICINE

Pretreatment with Haloperidol Reduces ^{123}I-FP-CIT Binding to the Dopamine Transporter in the Rat Striatum: An In Vivo Imaging Study with a Dedicated Small-Animal SPECT Camera

Susanne Nikolaus, Christina Antke, Konstantin Kley, Markus Beu, Andreas Wirrwar and Hans-Wilhelm Müller

J Nucl Med. 2009;50:1147-1152.
Published online: June 12, 2009.
Doi: 10.2967/jnumed.109.061952

The Journal of Nuclear Medicine is published monthly.
SNMMI | Society of Nuclear Medicine and Molecular Imaging
1850 Samuel Morse Drive, Reston, VA 20190.
(Print ISSN: 0161-5505, Online ISSN: 2159-662X)

SNMMI SOCIETY OF NUCLEAR MEDICINE AND MOLECULAR IMAGING